**International Journal of Applied Mathematics**

**Volume 38 No. 12s, 2025**

ISSN: 1311-1728 (printed version); ISSN: 1314-8060 (on-line version)

# MATHEMATICAL MODEL ARISING FROM THE ENCAPSULATION OF PHENYLALANINE AMINO ACID INSIDE SINGLE-WALLED CARBON NANOTUBES

**Hakim AL Garalleh*[a], Mou'ad A. Tarawneh[b], Mazen Garaleh[c] and Albara Alrawashdeh[a, c]**

a. Department of Mathematical Science, College of Engineering,
University of Business and Technology, Jeddah 21361, Saudi Arabia
Email[1]: h.algaralleh@ubt.edu.sa

b. Department of Physics, College of Science, Al-Hussein Bin
Talal University, P.O. Box 20, Ma'an 71110, Jordan.
Email[2]: moaath.tarawnah@ahu.edu.jo

c. Department of Chemistry and Chemical Technology, Faculty of Science,
Tafila Technical University, Tafila, 66110, Jordan.
Email[3]: mazen72_r@yahoo.com
Email[4]: a.alrawashdeh@ubt.edu.sa

Math. Subject Classification 2020: 82D10, 70G10

## Abstract

The combination between nanotechnology and biological studies has generated considerable interest in many potential applications, especially mechanisms of encapsulation and reactivity. The possibility of utilizing carbon nanodevices (CNDs) as transporters in various medical applications has led to a huge number of studies involving the realistic mechanism of geometries and the interaction between nanodevices and drugs, such as amino acids. Due to their huge potential, maximum loading and low solubility, new techniques have been developed for drug delivery system. The current work aims to investigate the mechanism of encapsulation of Phenylalanine (PHLNN) amino acid inside the single-walled carbon nanotubes (SWCNTs) varying in radii $r$. In our proposed model, the PHLNN is assumed to have two possible structures. Firstly, by using a discrete approach the PHLNN molecule can be splited into two parts: as an imidazole ring and a group of atoms as a spherical shell. Secondly, it can be considered as a cylindrical tube by using the continuum approximation. Here, we specify a certain shape for each of interacting molecules and also calculate the magnitude of interaction energy arising from PHLNN-SWCNTs interactions varying in radii $r$. Critical radius plays a crucial r in determining the acceptance and rejection of proposed amino acid inside an SWCNT. Particularly with respect to the financial aspect, carbon nanoparticle derivatives can be probably used as carriers and sensors conjugated with different drugs and amino acids because of their low manufacturing cost, ease of manipulation and synthesis as well as ability to maximum loading

Received: August 05, 2025

International Journal of Applied Mathematics

Volume 38 No. 12s, 2025

ISSN: 1311-1728 (printed version); ISSN: 1314-8060 (on-line version)

**Keywords:** Carbon nanodevices (CNDs), Single-walled carbon nanotubes (SWCNT), Phenylalanine amino acid (PHLNN), Encapsulation, Interaction energy, van der Waals interaction and Lennard-Jones potential.

## 1. Introduction

Nowadays, the revolution of nanotechnology continues and provides many environmental and beneficial tools that allow us to generate individual materials and molecules at the nanoscale for drug delivery applications. The terminology of nanotechnology had been first suggested by the physicist Richard Feynman in 1959, but it was first utilized in 1974 by Norio Taniguchi, a researcher at Tokyo University, who mentioned the ability of materials at the nanometer scale [1]. Particularly with respect to nanobiotechnology system arising from the combination between biology and nanotechnology, involving the schematic geometry of various biomolecules interacting with carbon nanostructures [2-5]. Nanobiotechnology field aims to investigate and study the transportation of bio-molecular system and also motivates scientists to develop and design new nanodevices by manipulating in their sizes, shapes, and chemical and electrical properties to enhance the efficacy of drugs delivered to the targeted tissues and cells [6-8].

The conception of nanotechnology has attracted much attention and generated considerable interest because of its intrinsic properties and unique geometric structures [9]. Carbon nanodevices have a huge potential for developing new techniques, especially for drug delivery systems, such as fullerene derivatives, and single- and multi-walled carbon nanotubes (SWCNTs and MWCNTs) [10]. These engineered nanodevices can be often used as carriers, anti-agents and sensors in various medicinal and biological applications [8,11-14]. Carbon nanostructures can be possibly combined with different biomolecules and drugs delivered into targeted areas by manipulating in their exceptional chemical and conductivity properties [15]. Long-term and recent studies have discussed the realistic mechanism of therapeutic agents, proteins and $\alpha$-amino acids conjugated fullerene derivatives and CNTs as transporters, sensors, inhibitors and antioxidant agents for drug delivery applications [16-20].

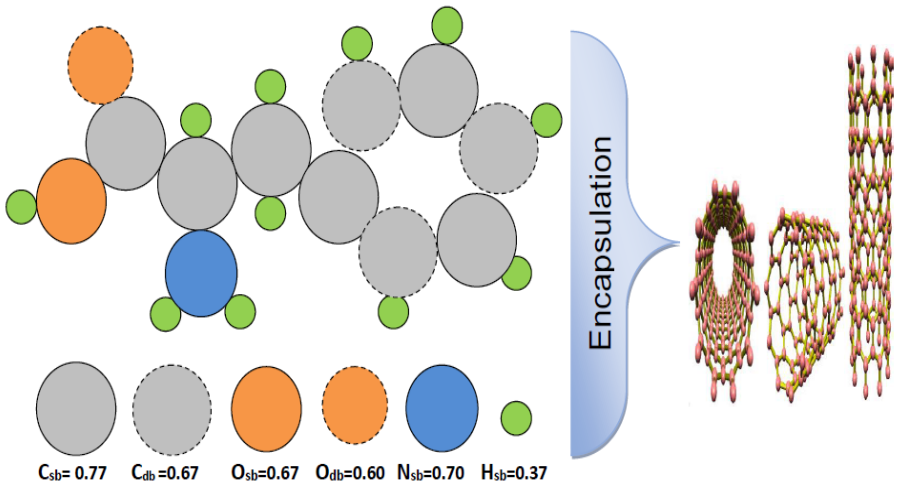


**Figure 1:** Schematic geometry of the PHLNN amino acid interacting with SWCNTs varying in radius $r$.

Received: August 05, 2025

Volume 38 No. 12s, 2025
ISSN: 1311-1728 (printed version); ISSN: 1314-8060 (on-line version)

Over the past few decades, the possibility of combination between different amino acids and carbon materials at the nanoscale sizes have been addressed such as L-Histidine, Alanine, Cystine and other $\alpha$-amino acids. The work of Roman et al. [18] who use the Density Functional (DF) method to investigate the ability of CNTs with variant diameters of approximately ~ 4 Å for adsorption of proteins and amino acids. Later, Ganji et al. [21] who calculate the potential energy arising from the encapsulation of Cysteine, PHLNN and Histidine amino acids interacting with the inner surface of SWCNT (13,0). In addition, Ganji's work has investigated the encapsulation of L-Histidine amino acid inside CNTs by using two different methods; Spanish Initiative for Electronic Simulations (SIESTA) and density Functional-Based Tight Binding Plus (DFTB+) [21]. Furthermore, the encapsulation of different amino acids, L-Histidine, Alanine and Cystine, inside the SWCNTs of various radii $r$ obtained as mathematical models to calculate the interaction energy arising from each sub-interaction and deduce the critical radius that would accept these biomolecules [22-24]. Most recent theoretical and experimental results indicate that these $\alpha$-amino acids were able to suck inside different CNTs with variant radii $r$ and also show that the minimum energies arising from [$\alpha$-amino acids]-SWCNTs interactions are in the range of approximately - 0.1 to - 0.8 $kcal/mol$.

The proposed model aims to identify the economic significance of using carbon nanostructures as transporters for drug delivery in terms of safety and non-toxicity. We also obtain a mathematical model to describe the possibility of adsorption of PHLNN molecule inside SWCNT of various radius $r$ (see Fig.1). PHLNN is classified as one of the significant and essential amino acid inside the human body (self-synthesized) with chemical formula $C_9H_{11}NO_2$. Its structure has a precursor for catecholamines which act as neurotransmitters, namely adrenalin-semi substances. PHLNN structure had been identified by Schulze and Barbieri in 1879 [25], but in 1881 was firstly synthesized from ammonia ($NH_3$), phenylacetaldehyde and hydrogen cyanide [25,26]. PHLNN has a vital role in metabolism and digestion especially for pregnant women who must control their blood test by keeping its level at the normal rate which is roughly 60 $\mu mol/L$. As known, the high or low levels of PHLNN at pregnant women could cause hepatic immaturity [27]. PHLNN amino acid is uniformly distributed to the different tissues in the human body by penetrating the blood-brain barriers and it can be found in three different forms D-PHLNN, L-PHLNN and DL-PHLNN [28].

This paper organized as: we briefly introduce the Lennard-Jones potential and van der Waals force then evaluate the total interaction energy by using a continuum approach and depending on the inner radius of nanotube. Next, we convert the biophysical application to a mathematical model by defining schematic geometry and specifying the certain shape for each interacting molecule. Followed by a discussion and analysis of our results in section 3. Finally, conclusions are given in the last section.

Received: August 05, 2025

International Journal of Applied Mathematics

Volume 38 No. 12s, 2025

ISSN: 1311-1728 (printed version); ISSN: 1314-8060 (on-line version)

**Table 1**: The Lennard-Jones constants (ϵ: Bond length; σ: Non-Bond distance; single bond: sb and double bond: db) [31].

| Interaction | $\varepsilon$ (Å) | $\sigma$ (Å) | Interaction | $\varepsilon$ (Å) | $\sigma$ (Å) |
|---|---|---|---|---|---|
| *H-H* | 0.74 | 2.886 | *O-H* | 0.96 | 3.193 |
| *O-O (sb)* | 1.48 | 3.500 | *O-O (db)* | 1.21 | 3.500 |
| *N-N* | 1.45 | 3.660 | *N-H* | 1.00 | 3.273 |
| *C-C (sb)* | 1.54 | 3.851 | *C-H* | 1.09 | 3.368 |
| *C-C (db)* | 1.34 | 3.851 | *C-O (sb)* | 1.43 | 3.675 |
| *C-O (db)* | 1.20 | 3.675 | *C-N* | 1.47 | 3.755 |
| *N-O* | 1.09 | 3.368 | *S-S* | 2.05 | 4.035 |
| *S-H* | 1.34 | 3.461 | *S-C* | 1.77 | 3.934 |

## 2. Method

### 2.1 Mathematical Model

Here, we obtain the biophysical application (See Fig.2) which describes the encapsulation of PHLNN amino acid into the interior cavity of the SWCNT with variant radii r. This proposed model is obtained mathematically by using the van der Waals force and Lennard-Jones potential. The Cartesian coordinate *(x, y, z)* used as a reference system to model each of the two interacting molecules. The non-bonded interaction energy obtained by summing the interaction energy (*E*) for each interacting atom,

$$E = \eta_c \, \eta_l \, \sum_i \sum_j \emptyset(\rho) \quad , \qquad (1)$$

where $\emptyset(\boldsymbol{\rho})$ is a potential function for atoms $\boldsymbol{i}$ and $\boldsymbol{j}$ at distance $\rho$. Here, we apply a discrete approach, and atoms are assumed to be uniformly distributed over the surfaces of the two interacting molecules. The double summation in Equation (1) can be replaced by a double integral, which average over the surface of each atom

$$E = \eta_c \, \eta_l \int \int \emptyset(\rho) \, d_{Sc} \, d_{Sl} \quad , \qquad (2)$$

where $\eta_c$ and $\eta_l$ are the atomic surface densities for the two molecular structures and the distance between the two interacting molecules denotes by $\rho$. The classical Lennard-Jones potential for two molecules at a distance $\rho$ apart can be given as

$$\emptyset(\rho) = \frac{-A}{\rho^6} + \frac{B}{\rho^{12}} \quad , \qquad (3)$$

where $A$ and $B$ are the attractive and repulsive constants, respectively. The Lennard-Jones potential and van der Waals interaction used as empirical combining laws, which are given by and, where $\varepsilon$ is the well depth and $\sigma$ is the van der Waals diameter [29,30], to calculate the physical parameters involved in this model; A = $4\varepsilon\sigma^6$ and B = $4\varepsilon\sigma^{12}$. The interaction energies calculated for the two proposed submodels.

Received: August 05, 2025

**International Journal of Applied Mathematics**

**Volume 38 No. 12s, 2025**

ISSN: 1311-1728 (printed version); ISSN: 1314-8060 (on-line version)

**Table 2**: Numerical values of the attractive and repulsive constants.

| Interaction | Attractive | Value ( $Å^6$ $kcal/mol$) | Repulsive | Value ( $Å^{12}x\ 10^3$ $kcal/mol$) |
|---|---|---|---|---|
| *C-C* | $A_{CC}$ | 22.63 | $B_{CC}$ | 65.533 |
| *H-C* | $A_{HC}$ | 17.16 | $B_{HC}$ | 31.729 |
| *N-C* | $A_{NC}$ | 41.26 | $B_{NC}$ | 115.661 |
| *O-C* | $A_{OC}$ | 33.79 | $B_{OC}$ | 83.246 |
| *S-C* | $A_{SC}$ | 139.04 | $B_{SC}$ | 522.516 |
| *O-H* | $A_{OH}$ | 9.41 | $B_{OH}$ | 9.972 |
| *N-H* | $A_{NH}$ | 11.70 | $B_{NH}$ | 14.383 |
| *CNT* | $A_{CNT}$ | 17.40 | $B_{CNT}$ | 29.000 |
| *An imidazole Ring (R)* | $A_R$ | 20.14 | $B_R$ | 50.167 |
| *Spherical shell (b)* | $A_b$ | 19.87 | $B_b$ | 45.595 |
| *Cylindrical group of atoms ($r_d$)* | $A_d$ | 21.22 | $B_d$ | 50.670 |
| *Ring-CNT* | $A_{R-CNT}$ | 18.77 | $B_{R-CNT}$ | 39.584 |
| *Sphere-CNT* | $A_{b-CNT}$ | 18.64 | $B_{b-CNT}$ | 37.298 |
| *Cylindrical group -CNT* | $A_{d-CNT}$ | 19.32 | $B_{d-CNT}$ | 39.835 |

**.2 Discrete approach model: PHLNN modelled as an imidazole ring and aspherical shell interacting with an SWCNT**

By using the discrete approximation, we determine the PHLNN-SWCNT interaction in two parts as shown in Figure 3(i) and (ii). Firstly, we consider the 5 hydrogen and 6 carbon atoms assumed to be a ring of imidazole group of radius R = $\sigma_{CC} + \sigma_{CH}$ interacting with a single-walled carbon nanotube of radius $r$. The nanotube is assumed to be cylindrical tube that can be parameterized by $(rcos\theta, rsin\theta, z)$ where $r \in (0,1)$, $z \in (-\infty, \infty)$ and $\theta \in [-\pi, \pi]$. The ring of imidazole group is assumed to be located at $(Rcos\psi, 0, Rsin\psi + z_0)$, where $R$ is the radius of the inner ring, $\psi \in [0, 2\pi]$ and the distance $\rho_1$ between the inner ring and the nanotube tube is ${\rho_1}^2 = (rcos\theta - Rcos\psi)^2 + (rsin\theta)^2 + (z - Rsin\psi - z_0)^2$. From the work of Tran-duc et al. [32] (special case: $\epsilon = 0$, $R$ : constant, $\phi$ is variant), the interaction energy between the ring and the SWCNT (see Fig. 3(i)) is given by

$$E_1 = \eta_c \eta_R \int\int \emptyset(\rho)\, d_{Sc}\, d_{SR} = \eta_c \eta_R(-A J_3 + B J_6)\ , \qquad (4)$$

where $\eta_c$ and $\eta_R$ are the atomic surface densities for a carbon nanotube and line density of the ring, respectively. We note that $d_{Sc} = r\, dz$ and $d_{SR} = R\, d\psi$. Here, the integral $J_n$ is defined by

Received: August 05, 2025 

**International Journal of Applied Mathematics**

**Volume 38 No. 12s, 2025**

ISSN: 1311-1728 (printed version); ISSN: 1314-8060 (on-line version)

$$J_n = r\,R \int_0^{2\pi}\int_0^{2\pi}\int_{-\infty}^{\infty} \frac{1}{{\rho_1}^{2n}}\; dz\; d\theta\; d\psi\,. \qquad (5)$$

Secondly, 3 carbon, 2 oxygen, 1 nitrogen and 6 hydrogen atoms forming a spherical shell of radius $b = (\sigma_{HN} + \sigma_{CC} + \sigma_{CO} + \sigma_{CO})/2$ interacting with an SWCNT with variant radii $r$. The spherical shell of radius b assumed to be located at $(bcos\theta sin\phi, rsin\theta sin\phi, bcos\phi)$, where $\theta \in [-\pi, \pi]$, $\phi \in [-\pi/2, \pi/2]$ and the distance $\rho 2$ between the spherical molecule and a typical point $P$ on the cylindrical tube is $\rho_2 2 = (rcos\theta - bcos\theta sin\phi)2 + (rsin\theta - bsin\theta sin\phi)2 + (z - bcos\phi)2$. From the work of Cox et al. [33], the interaction energy between a spherical molecule and a typical point $P$ on the cylindrical tube can be given as

$$E_2 = \eta_b\,\pi\,b \int\int\int \left[\frac{A}{2}\left(\frac{1}{\rho_3(\rho_3+b)^4} - \frac{1}{\rho_3(\rho_3-b)^4}\right) - \frac{B}{5}\left(\frac{1}{\rho_3(\rho_3+b)^{10}} - \frac{1}{\rho_3(\rho_3-b)^{10}}\right)\right] dV$$

$$= \eta_c\,\pi\,b \int_{-L/2}^{L/2}\int_{-\pi}^{\pi}\int_0^1 r^2 \left[\frac{A}{2}\left(\frac{1}{\rho_3(\rho_3+b)^4} - \frac{1}{\rho_3(\rho_3-b)^4}\right) - \frac{B}{5}\left(\frac{1}{\rho_3(\rho_3+b)^{10}} - \frac{1}{\rho_3(\rho_3-b)^{10}}\right)\right] dr\; d\theta\; dz, \quad (6)$$

where $\eta_b$ is the atomic surface density of the spherical shell and $dV = r^2\; dr\; d\theta\; dz$ is the element volume. We then gather all sub-interactions to evaluate the magnitude of total interaction energy that would be given as:

$$E = E_1 + E_2.$$

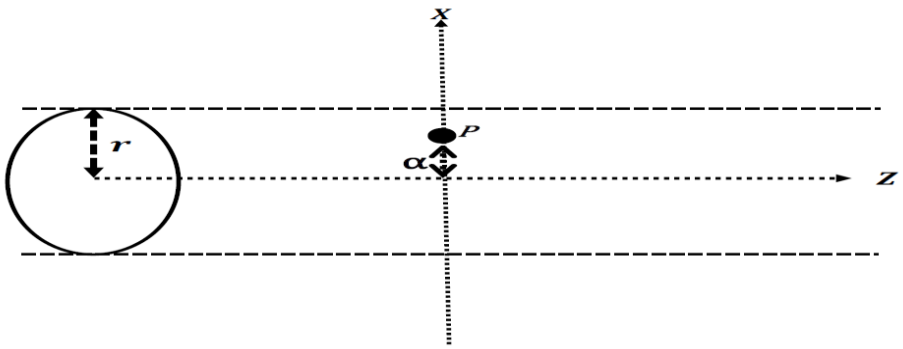


**Figure 2:** Schematic illustration of the interaction between an atom (PHLNN molecule) at point $P$ (off-setting from the central-axis by a distance $\alpha$) and a SWCNT of radius $r$.

International Journal of Applied Mathematics

Volume 38 No. 12s, 2025

ISSN: 1311-1728 (printed version); ISSN: 1314-8060 (on-line version)

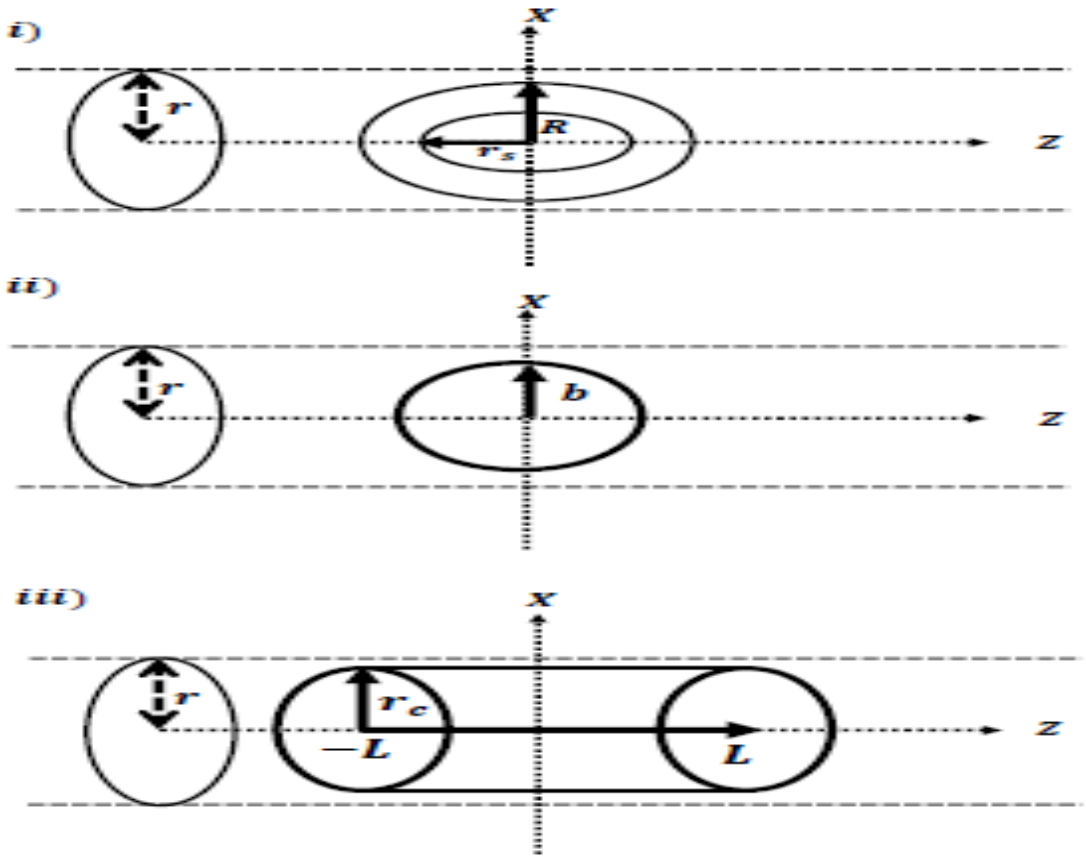


**Figure 3:** Possible configurations of PHLNN molecule (with different subcomponents: each comprising specific atoms): i) An imidazole ring of radius $R$, ii) spherical shell (group of atoms) of radius $b$ and iii) a cylinder group of atoms (finite in length) of radius $r_d$, each interacting with an SWCNT of radius $r$ along the z-axis.

### 2.3 Continuum approach model: PHLNN modelled as a cylindrical shell and aspherical shell interacting with an SWCNT

Here, we assume a group of 9 carbon, 1 nitrogen, 2 oxygen and 11 hydrogen atoms as a cylindrical shell of radius $\mathrm{r_d} = (\sigma\mathrm{CC} + \sigma\mathrm{CO} + \sigma\mathrm{CN} + \sigma\mathrm{CH})/2$ and length $L = \sigma_{OH} + \sigma_{CO} + 5\sigma_{CC} + \sigma_{CH}$. This cylinder is assumed to be located at $(r_d\, cos\theta 1, r_d\, sin\theta 1, tcos\phi + z0)$ and $t \in [0, (\sigma_{CC} + \sigma_{CO} + \sigma_{CN} + \sigma_{CH})/2]$, where the distance $\rho_3$ between the nanotube of radius r and the cylindrical group of radius $\mathrm{r_c}$ (see Figure 3(iii)) is given by ${\rho_3}^2 = (rcos\theta - r_d\, cos\theta 1)^2 + (rsin\theta - r_d\, sin\theta 1)^2 + (z - (tcos\phi + z0))^2$. From the work of Cox et al. [34], the interaction energy arising from the cylindrical tube-SWCNT interaction is given by

$$E_3 = \eta_c\, \eta_d\, (-A\, T_3 + B\, T_6) \quad , \tag{8}$$

where $\eta_d = (6/\text{surface area of the cylindrical group})$ is the atomic surface density for the cylindrical tube and $T_n$ $(n = 3\ and\ 6)$ is given by

Received: August 05, 2025

International Journal of Applied Mathematics

Volume 38 No. 12s, 2025

ISSN: 1311-1728 (printed version); ISSN: 1314-8060 (on-line version)

$$T_n = \int_{-(\sigma_{CC}+\sigma_{CO}+\sigma_{CN}+\sigma_{CH})/2}^{(\sigma_{CC}+\sigma_{CO}+\sigma_{CN}+\sigma_{CH})/2} \int_0^{2\pi} \int_0^{2\pi} \int_{-\infty}^{\infty} \frac{r}{{\rho_2}^2}\, dz\, d\theta\, d\theta_1\, dt \quad . \tag{9}$$

### 2.4 Acceptance of PHLNN inside an SWCNT

To demonstrate the encapsulation of the PHLNN amino acid inside an SWCNT, we first need to determine the acceptance energy. We then evaluate the acceptance energy moving from $-\infty$ to $z_0$ to determine if the PHLNN molecule will be sucked into a cylindrical SWCNT. From the work of Cox et al. [34] a molecule is accepted inside an SWCNT if the acceptance energy ($A_r$) is greater than zero, which is given by

$$A_r = \int_{-\infty}^{z_0} \frac{dE}{dz}\, dz = E(z_0) - E(-\infty) \quad , \tag{10}$$

noting that $z_0$ is the root of equation $\partial E/\partial z = 0$, which is the point where the molecule is about to enter the nanotube.

**Table 3**: Physical parameters for SWCNTs and other components: configuration, dimensions and atomic surface density

| Configuration | Dimenions (Å) | ValueAtomic surface density ( $Å^{-2}$) |
|---|---|---|
| SWCNT(9,7) | $r = 8.571$ | 0.381 |
| SWCNT(10,6) | $r = 8.833$ | 0.381 |
| SWCNT(12,4) | $r = 9.027$ | 0.381 |
| SWCNT(12,5) | $r = 9.468$ | 0.381 |
| SWCNT(11,8) | $r = 10.344$ | 0.381 |
| SWCNT(10,10) | $r = 10.843$ | 0.381 |
| SWCNT(13,7) | $r = 10.994$ | 0.381 |
| An imidazole ring (R) | $R = 7.219$ | 0.015 |
| Spherical shell (b) | $b = 7.278$ | 0.008 |
| Cylindrical group of atoms ($r_d$) | $r_d = 7.235$ and $L = 29.49$ | 0.009 |

## 3. Results and Discussion

In this section, we adopt the discrete-continuum approach and the Lennard-Jones potential together to evaluate the interaction energy arising from the encapsulation of PHLNN amino acid inside an SWCNT of radius r. The well-depth ϵ and van der Waals diameter σ are shown as in Table 1. The attractive and repulsive constants, (A = $4\varepsilon\sigma^6$) and (B = $4\varepsilon\sigma^{12}$), are calculated by using the empirical laws combining the well-depth ϵ and the van der Waals diameter σ and given in Table 2. We calculate the atomic densities from dividing the number of atoms for each proposed configuration by the surface area or volume of the assumed structure imidazole ring ($\eta_R$), spherical shape ($\eta_b$), group of atoms as cylindrical tube ($\eta_d$) and cylindrical tube ($\eta_c$)

Received: August 05, 2025

**International Journal of Applied Mathematics**

**Volume 38 No. 12s, 2025**

ISSN: 1311-1728 (printed version); ISSN: 1314-8060 (on-line version)

which are $\eta_R$ = number of atoms/$(4\pi rR)$, $\eta_b$ = number of atoms/$(4\pi b^2)$, $\eta_s$ = number of atoms/$(2\pi\, r_d L)$ and $\eta_c$ = number of atoms/$(2\pi rL)$, respectively, as shown in Table 3.

Next, the interaction energy for each configuration interacting individually with an SWCNT of radius $r$ evaluated and plotted along the $z$-axis for both proposed configurations by using the MAPLE package. Specifying the certain shape for each interacting structural molecule is very important to calculate the minimum energy for each sub-interaction by performing the surface or volume integral of Lennard-Jones potential over the nanotube as shown in Figs. 4 to 9. By assuming the SWCNT as an infinite cylindrical nanotube (well-defined), and by considering the (9,7), (10,6), (12,4), (12,5), (11,8), (10,10) and (13,7) SWCNTs which have radii in the range of $8.571 \leq r \leq$ 10.994 as shown in Table 3 to determine the encapsulation of PHLNN amino acid inside these SWCNTs. The minimum energy for each orientation obtained is based on the equilibrium position of the PHLNN molecule which is placed away from the interior wall of SWCNT. From Figures 4 to 11, we determine the minimum radius of SWCNT $r$ for each proposed configuration that will completely accept the PHLNN amino acid and find out that PHLNN molecule as 2-components and finite cylindrical tube are stable that would be accepted inside the nanotube when $r$ are greater than 9.03 and 9.46 Å, respectively. In addition, we note that there is a minimal difference in the magnitude of minimum energy for the two proposed sub-models and the SWCNT(10,10) is the most favorable physical nanotube with radius of 10.843 Å (see Fig. 8) which has the lowest interaction energy arising from the PHLNN as 2-components and PHLNN as a cylinder group of atoms (Figs. 10 and 11) interacting with SWCNTs with variant radii $r$ of roughly -1.15 and -1.08 *kcal/mol*, respectively.

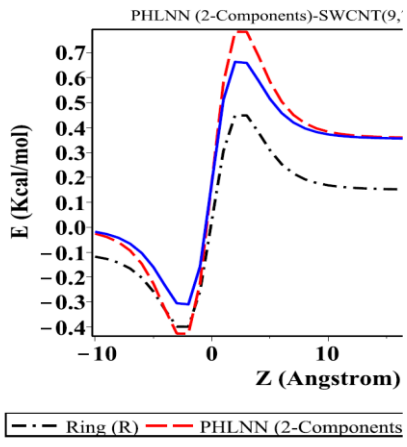


**Figure 4:** Interaction energy from the PHLNN amino aci with SWCNT(9,7) along the

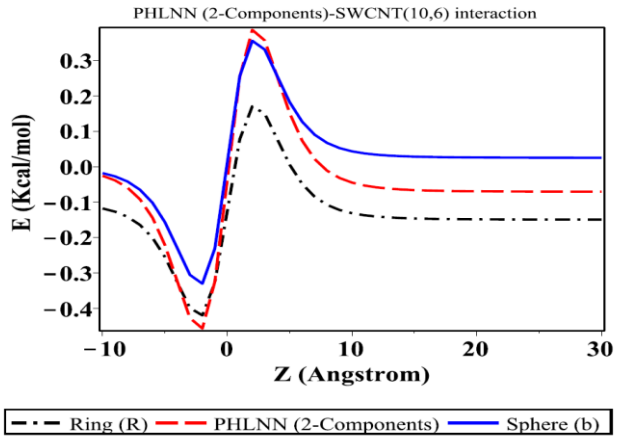


**Figure 5:** Interaction energy ($E$) arising from the PHLNN amino acid interacting with SWCNT(10,6) along the $z$-axis.

Received: August 05, 2025

**International Journal of Applied Mathematics**

**Volume 38 No. 12s, 2025**

ISSN: 1311-1728 (printed version); ISSN: 1314-8060 (on-line version)

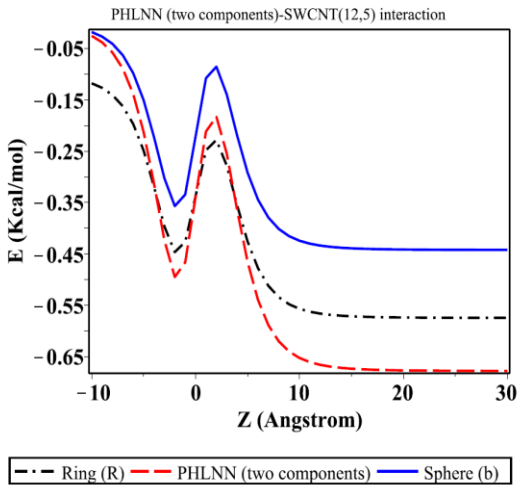


**Figure 6:** Interaction energy ($E$) arising from the PHLNN amino acid interacting with SWCNT(12,5) along the $z$-axis.

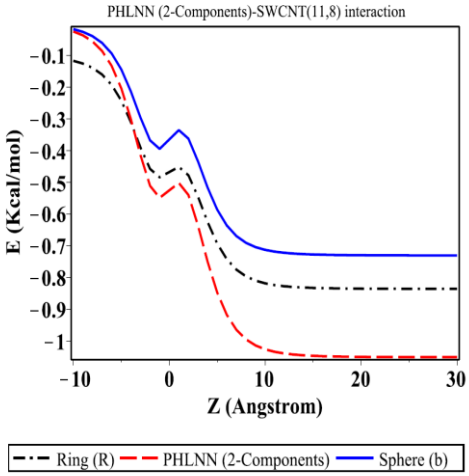


**Figure 7:** Interaction energy ($E$) arising from the PHLNN amino acid interacting with SWCNT(11,8) along the $z$-axis.

ur :or

$R$ and a sphere of radius $b$ in the range of $-10 \leq r \leq 30$ (Figs. 4 to 11), we then gather all the two pairs of interactions to determine the magnitude of total interaction energy (Eq. 7). The equilibrium position is the physical distance between each component of PHLNN molecule and the inner surface of an SWCNT, where the interaction

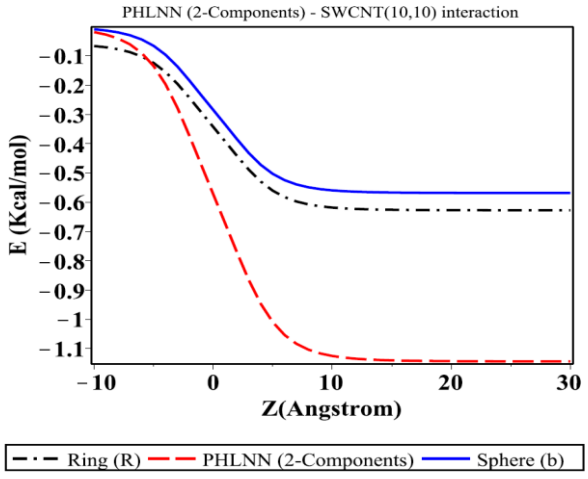


**Figure 8:** Interaction energy ($E$) arising from the PHLNN amino acid interacting with SWCNT(10,10) along the $z$-axis.

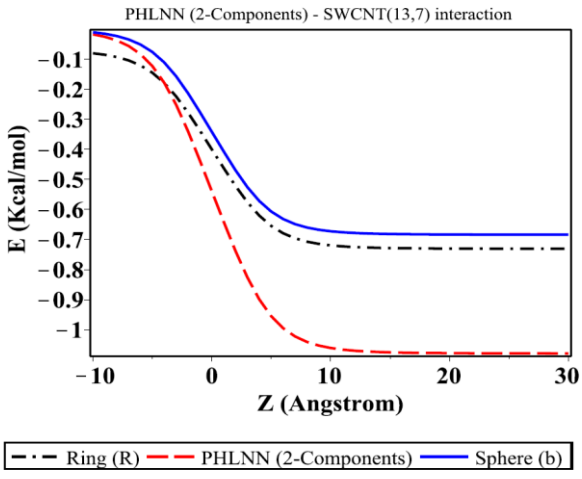


**Figure 9:** Interaction energy ($E$) arising from the PHLNN amino acid interacting with SWCNT(13,7) along the $z$-axis.

Received: August 05, 2025

**International Journal of Applied Mathematics**

**Volume 38 No. 12s, 2025**

ISSN: 1311-1728 (printed version); ISSN: 1314-8060 (on-line version)

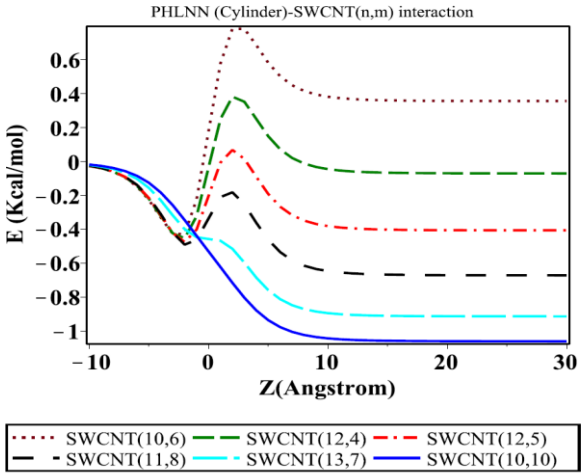


**Figure 10:** Interaction energy ($E$) arising from the PHLNN amino acid as cylinder group of atoms interacting with SWCNTs varying in radii $r$ along the $z$-axis.

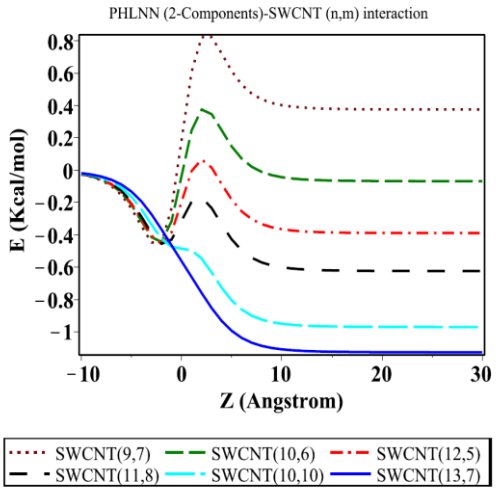


**Figure 11:** Interaction energy ($E$) arising from the PHLNN amino acid 2-components interacting with SWCNTs varying in radii $r$ along the $z$-axis.

energy obtained as its minimum. As in Figure 12, we also plot the relationship between the interaction energy and radius of nanotube $r$. The critical radius $r$ is deduced and plays a significant role in determining the magnitude of interaction energy, we note that the PHLNN as 2-components is more preferable inside an SWCNT than that of PHLNN as a cylindrical tube of radius $r_d$. This is attributed to the smaller volumes of an imidazole ring of radius $r$ and a sphere of radius $b$ that require smaller radii $r$. We also observe that the interaction energy associated with the encapsulation of PHLNN as 2-components is in the range of $-0.05 \leq E \leq -1.15$ compared with that of PHLNN as a cylinder group is in the range of $-0.09 \leq E \leq -1.08$ (see Fig. 12). For both configurations with similar trend, our numerical results indicate that PHLNN molecule as 2-components and a cylinder group will be unstable and repulsive inside an SWCNT when $r$ is smaller than 9.027 and 9.468 Å as shown in Table 4 (see Fig. 13), respectively. For instance, Work of Zheng and Ganji who confirm that the adsorption of different amino acid inside an SWCNT of various radius $r$ is practically carried out [21,35] and Roman's work who also investigate the nucleic amino acids sucked into SWCNT(10,0) [18] as well as Al Garalleh's who have studied the possibility of encapsulation of Cystine, L-Histidine and Alanine amino acids inside SWCNTs of variant radii $r$ [22-24]. All their experimental results consistently agree with our numerical results and also focus on determining the critical radius because of having a crucial role in determining the magnitude of interaction energy for each proposed configuration.

Finally, the acceptance energy of the PHLNN amino acid evaluated and plotted for the two proposed sub-models by using Eq. (10) as a function of the SWCNT $r$. The critical radius $r$ of

Received: August 05, 2025

**International Journal of Applied Mathematics**

**Volume 38 No. 12s, 2025**

ISSN: 1311-1728 (printed version); ISSN: 1314-8060 (on-line version)

the SWCNT for the acceptance of PHLNN molecule can be also deduced (Fig. 13). We comment that the acceptance of PHLNN molecule inside an SWCNT occurs when $A_r$ is greater than zero. The 2-components PHLNN would be spontaneously accepted when $r$ exceeds 9.03±0.02 Å, while the acceptance of PHLNN as a cylindrical tube inside an SWCNT when $r$ exceeds 9.45±0.01 Å. The smaller volume of 2-components configuration compromising PHLNN would be more likely to reside inside the nanotube compared with PHLNN as a cylinder group. We contend that the realistic mechanism of encapsulation for both proposed sub-models are carried out, i.e., show the acceptance and stability for a PHLNN molecule inside SWCNTs with $r$ in the range of $9.027 \leq r \leq 10.995$ Å. Long-term studies confirm and support the obtained results above, work of Salvador-Morales et al. [12], Cheng et al. [14], Roman et al. [18], AL Garalleh et al. [22-24] and Zheng et al. [35], demonstrated that the possibility of encapsulation of different $\alpha$-amino acids and proteins inside the graphite sheets and CNTs by using different methods, numerically and experimentally, is carried out.

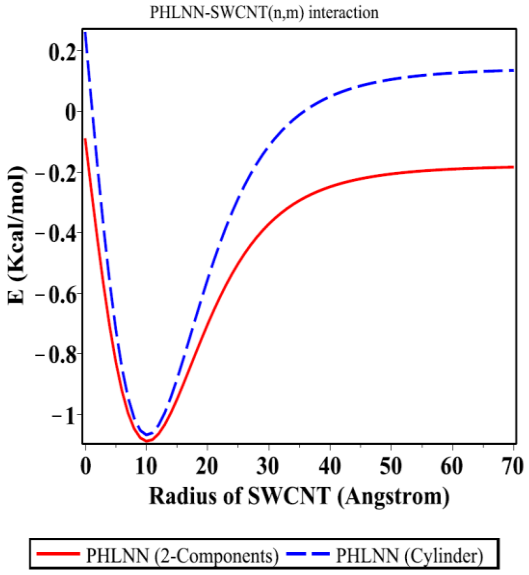


**Figure 12:** The relationship between the interaction energy ($E$) arising from the PHLNN amino acid interacting with SWCNTs and the radius $r$ of SWCNT.

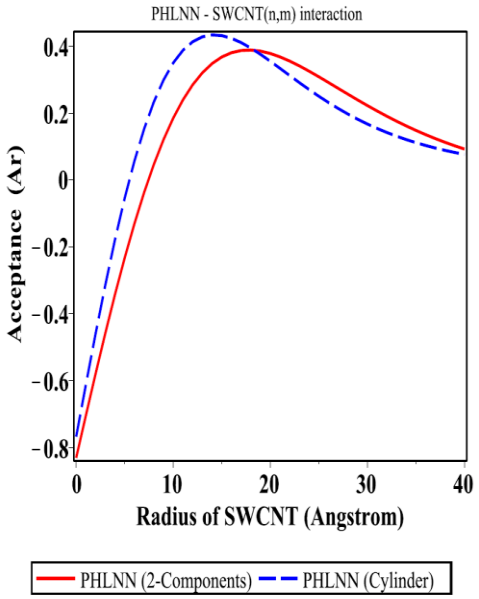


**Figure 13:** The relationship between the acceptance energy and the radius $r$ of SWCNT.

In the term of financial significance, CNPs have financially distinct properties that has recently generated a great interest because of low production cost and high effectiveness which has led to increasing the demand within industries to develop new nanodevices (NDs) for biological and medical purposes [36,37]. They are also considered as friendly environmental materials due to their intrinsic characters such as lighter, stronger and non-toxic; this globally motivates the researchers to use the fictionalized CNPs in many real-life applications, particularly with respect to nanomedical applications [38-40]. In addition, production of CNTs on a commercial

Received: August 05, 2025

Volume 38 No. 12s, 2025
ISSN: 1311-1728 (printed version); ISSN: 1314-8060 (on-line version)

scale will have a great impact on obtaining a continuous process on high-purity, high-yield, and low-production cost of nanomaterials fabrication [36,40].

**Table 4**: Physical parameters for SWCNTs and other components: proposed configuration, critical radius, dimensions and minimum energy

| Proposed configuration | Critical radius $r$ (Å) | Favorable SWCNT(m,n) | Minimum interaction energy (kcal/mol) |
|---|---|---|---|
| Imidazole Ring (R) | $r \geq 8.833 \pm 0.02$ | SWCNT(10,10) | $-0.63 \pm 0.02$ |
| Sphere structure (b) | $r \geq 9.027 \pm 0.03$ | SWCNT(10,10) | $-0.52 \pm 0.02$ |
| PHLNN as 2-components | $r \geq 9.027 \pm 0.03$ | SWCNT(10,10) | $-1.08 \pm 0.01$ |
| PHLNN as a cylinder | $r \geq 9.468 \pm 0.02$ | SWCNT(10,10) | $-1.15 \pm 0.01$ |

## 4. Conclusions

In brief, the biophysical application adopted in this proposed work describes the mechanism of encapsulation of PHLNN amino acid inside an SWCNT as a mathematical model. The PHLNN-SWCNT interaction evaluated by specifying the certain shape for each configuration interacting with an SWCNT varying in radii *r*. The continuum-discrete approach and classic Lennard-Jones potential adopted to evaluate the potential energy arising from the PHLNN-SWCNT interaction where SWCNT is assumed to be uniformly characterized and well-defined. Deducing the critical radius of SWCNT *r* plays a crucial role in determining the acceptance of PHLNN inside the SWCNT. Based on the numerical results obtained from the current work, we find out that the PHLNN molecule would practically be accepted when *r* =9.45 Å (SWCNT(12,5)) for the two proposed sub-models and also determine the minimum energy arising from the PHLNN-SWCNT interaction as two components ,each configuration interacts individually with the inner surface of SWCNT then gathers the two pair interactions, is roughly -1.15 when *r* =10.84$\pm$0.02 Å which is greater than that of PHLNN-SWCNT interaction as cylinder of group atoms (continuum approach) of approximately -1.08 *kcal/mol* (see Figs. 4 to 11). In addition, we notice that the SWCNT (10,10) is the most favorable nanotube for the two proposed sub-models and deducing the critical radius *r* has a major role in determining the minimum energy and the acceptance of PHLNN amino acid inside an SWCNT of various radius *r*.

Furthermore, we note that the PHLNN molecule, as 2-components and a cylindrical tube, is rejected and unstable inside the SWCNT of radius $r < 9.03$ and $r < 9.45$, respectively, and also evaluate and plot the relationship between the acceptance energy and the radius of SWCNT *r*.

Received: August 05, 2025

Volume 38 No. 12s, 2025

ISSN: 1311-1728 (printed version); ISSN: 1314-8060 (on-line version)

As shown in Figures 12 and 13, it is noticeable that PHLNN molecule as two components is more acceptable inside the SWCNT than PHLNN as a cylindrical tube with a minimal difference in the magnitude of acceptance energy ($A_r$). Overall, our numerical results obtained from the PHLNN-SWCNTs interactions are roughly in the range of -0.05 to -1.15 *kcal/mol* which are consistent and in excellent agreement with Ganji's work et al. [21] who shows that the encapsulation of different amino acid inside SWCNTs are possible and calculates the magnitude of interaction energies approximately in the range of -0.1 to -0.8 *kcal/mol* and also with the long-term studies which have experimentally addressed that the $\alpha$-amino acids, peptides and proteins as bio-sensors inside graphene sheets and the CNTs, especially when $r >$ 3.75 Å [12-14,18,22-24,35,41,42]. We note that there is a minimal difference in the magnitude of minimum energy arising from our proposed model in the range of -0.05 to -1.15 *kcal/mol* which is greater than that of Ganji's work of roughly -0.1 to -0.8 *kcal/mol*. This is attributed to the existence of energetic barriers and other physiological conditions, whilst our model is well-defined and characterized with no energetic barriers. Manipulating in the structural and conductivity properties of carbon nanomaterials has offered a unique opportunity to find nano-devices that could be used in many bioengineering and biomedical applications. In term of health and economic importance, stronger, lighter and thinner nanodevices are effectively worthier than the commercial tools because of high safety, non-toxic and low production cost.

**Acknowledgment**

The authors acknowledge that this project was funded by the Deanship of Scientific Research (DSR), University of Business and Technology, Jeddah. The authors, therefore, gratefully acknowledge the DSR technical and financial support.

**Funding**

This project was funded by the Deanship of Scientific Research (DSR), University of Business and Technology, Jeddah 21361, Saudi Arabia.

**Conflict of Interest**

Has no conflict of Interest.

**Data Availability Statement**

This article does not contain any studies with animals performed by any of authors.

**Author Contribution Statement**

The authors have equally written the proposed model, introduction, the numerical results, the conclusions besides reviewed the data analysis including the statistical errors.

## References

[1] Dilmaçünal, T., 2017. Intelligent Systems in the Food Packaging Industry: Contaminant Sensors and Security/Anticounterfeiting Devices. In Nanotechnology Applications in Food, pp.287-306. Academic Press, USA.

Received: August 05, 2025 

Volume 38 No. 12s, 2025

ISSN: 1311-1728 (printed version); ISSN: 1314-8060 (on-line version)

[2] Fakruddin, M., Hossain, Z. and Afroz, H., 2012. Prospects and applications of nanobiotechnology: a medical perspective. Journal of Nanobiotechnology, 10(1), p.31.

[3] Jain, K.K., 2007. Applications of nanobiotechnology in clinical diagnostics. Clinical chemistry, 53(11), pp.2002-2009.

[4] Hötzer, B., Medintz, I.L. and Hildebrandt, N., 2012. Fluorescence in nanobiotechnology: sophisticated fluorophores for novel applications. Small, 8(15), pp.2297-2326.

[5] Jain, K.K., 2008. Nanomedicine: application of nanobiotechnology in medical practice. Medical Principles and Practice, 17(2), pp.89-101.

[6] Ono, T., Fujimoto, Y. and Tsukamoto, S., 2012. First-principles calculation methods for obtaining scattering waves to investigate transport properties of nanostructures. Quantum Matter, 1(1), pp.4-19.

[7] Tüzün, B. and Erkoç, S., 2012. Structural and electronic properties of unusual carbon nanorods. Quantum Matter, 1(2), pp.136-148.

[8] Pantarotto, D., Partidos, C.D., Graff, R., Hoebeke, J., Briand, J.P., Prato, M. and Bianco, A., 2003. Synthesis, structural characterization, and immunological properties of carbon nanotubes functionalized with peptides. Journal of the American Chemical Society, 125(20), pp.6160-6164.

[9] Satvekar, R.K., Tiwale, B.M. and Pawar, S.H., 2014. Emerging trends in medical diagnosis: a thrust on nanotechnology. Med. Chem., 4, pp.407-416.

[10] Vardharajula, S., Ali, S.Z., Tiwari, P.M., Eroğlu, E., Vig, K., Dennis, V.A. and Singh, S.R., 2012. Functionalized carbon nanotubes: biomedical applications. International Journal of Nanomedicine, 7, pp.5361-2374.

[11] Pantarotto, D., Partidos, C.D., Hoebeke, J., Brown, F., Kramer, E.D., Briand, J.P., Muller, S., Prato, M. and Bianco, A., 2003. Immunization with peptide-functionalized carbon nanotubes enhances virus-specific neutralizing antibody responses. Chemistry and Biology, 10(10), pp.961-966.

[12] Salvador-Morales, C., Flahaut, E., Sim, E., Sloan, J., Green, M.L. and Sim, R.B., 2006. Complement activation and protein adsorption by carbon nanotubes. Molecular immunology, 43(3), pp.193-201.

[13] Liu, G.R., Cheng, Y., Mi, D. and Li, Z.R., 2005. A study on self-insertion of peptides into single-walled carbon nanotubes based on molecular dynamics simulation. International Journal of Modern Physics C, 16(08), pp.1239-1250.

[14] Cheng, Y., Liu, G.R., Li, Z.R. and Lu, C., 2006. Computational analysis of binding free energies between peptides and single-walled carbon nanotubes. Physica A: Statistical Mechanics and its Applications, 367, pp.293-304.

Received: August 05, 2025 

Volume 38 No. 12s, 2025

ISSN: 1311-1728 (printed version); ISSN: 1314-8060 (on-line version)

[15] Lin, Y., Taylor, S., Li, H., Fernando, K.S., Qu, L., Wang, W., Gu, L., Zhou, B. and Sun, Y.P., 2004. Advances toward bioapplications of carbon nanotubes. Journal of Materials Chemistry, 14(4), pp.527-541.

[16] Balavoine, F., Schultz, P., Richard, C., Mallouh, V., Ebbesen, T.W. and Mioskowski, C., 1999. Helical crystallization of proteins on carbon nanotubes: a first step towards the development of new biosensors. Angewandte Chemie International Edition, 38(13-14), pp.1912-1915.

[17] Allen O áHill, H., 1995. Immobilization of small proteins in carbon nanotubes: high-resolution transmission electron microscopy study and catalytic activity. Journal of the Chemical Society, Chemical Communications, (17), pp.1803-1804.

[18] Roman, T., Dino, W.A., Nakanishi, H. and Kasai, H., 2006. Amino acid adsorption on single-walled carbon nanotubes. The European Physical Journal D-Atomic, Molecular, Optical and Plasma Physics, 38(1), pp.117-120.

[19] An, Y.Z., Chen, C.H.B., Anderson, J.L., Sigman, D.S., Foote, C.S. and Rubin, Y., 1996. Sequence-specific modification of guanosine in DNA by a $C_{60}$-linked deoxyoligonucleotide: evidence for a non-singlet oxygen mechanism. Tetrahedron, 52(14), pp.5179-5189.

[20] Krusic, P.J., Wasserman, E., Keizer, P.N., Morton, J.R. and Preston, K.F., 1991. Radical reactions of $C_{60}$. Science, 254(5035), pp.1183-1185.

[21] Ganji, M.D., 2010. Calculations of Encapsulation of Amino Acids Inside the (13,0) Single-walled Carbon Nanotube. Fullerenes, nanotubes and carbon nanostructures, 18(1), pp.24-36.

[22] Garalleh, H.A., 2017. Modeling of encapsulation of Cystine amino acid inside a single-walled carbon nanotube. Materials Express, 7(5), pp.389-397.

[23] Garalleh, H.A., Thamwattana, N., Cox, B.J. and Hill, J.M., 2016. Encapsulation of L-Histidine amino acid inside single-walled carbon nanotubes. Journal of Biomaterials and Tissue Engineering, 6(5), pp.362-369.

[24] Al Garalleh, H., Garaleh, M. and Alabadleh, G., 2019. Mathematical model for the encapsulation of Alanine amino acid inside a single-walled carbon nanotube. Adsorption, pp.1-9.

[25] Thorpe, T.E. and Whiteley, M.A., 1912. A dictionary of applied chemistry Vol. 2, pp. 708-709, Longmans, Green and Company Ltd.

[26] Plimmer, R.H.A. and Hopkins, F.G., 2010. The chemical composition of the proteins. Monographs on biochemistry. Part I. Analysis.

[27] Sprenger, G.A., 2006. Aromatic amino acids. In Amino acid biosynthesis-pathways, regulation and metabolic engineering (pp. 93-127). Springer, Berlin, Heidelberg.

Received: August 05, 2025 

Volume 38 No. 12s, 2025
ISSN: 1311-1728 (printed version); ISSN: 1314-8060 (on-line version)

[28] Christianson, D.W., Mangani, S., Shoham, G. and Lipscomb, W.N., 1989. Binding of D-phenylalanine and D-tyrosine to carboxypeptidase A. Journal of Biological Chemistry, 264(22), pp.12849-12853.

[29] Cottrell, T.L., 1958. The strengths of chemical bonds. Butterworths Scientific Publications.

[30] Hirschfelder, J.O., Curtiss, C.F., Bird, R.B. and Mayer, M.G., 1964. Molecular theory of gases and liquids (Vol. 165). New York: Wiley.

[31] Rappé, A.K., Casewit, C.J., Colwell, K.S., Goddard III, W.A. and Skiff, W.M., 1992. UFF, a full periodic table force field for molecular mechanics and molecular dynamics simulations. Journal of the American chemical society, 114(25), pp.10024-10035.

[32] Tran-Duc, T., Thamwattana, N. and Hill, J.M., 2011. Orientation of a benzene molecule inside a carbon nanotube. Journal of mathematical chemistry, 49(6), pp.1115-1127.

[33] Cox, B.J., Thamwattana, N. and Hill, J.M., 2008. Mechanics of nanotubes oscillating in carbon nanotube bundles. Proceedings of the Royal Society A: Mathematical, Physical and Engineering Sciences, 464(2091), pp.691-710.

[34] Cox, B.J., Thamwattana, N. and Hill, J.M., 2007. Mechanics of atoms and fullerenes in single-walled carbon nanotubes. I. Acceptance and suction energies. Proceedings of the Royal Society A: Mathematical, Physical and Engineering Sciences, 463(2078), pp.461-477.

[35] Zheng, J., Song, W., Wang, L., Lu, J., Luo, G., Zhou, J., Qin, R., Li, H., Gao, Z., Lai, L. and Li, G., 2009. Adsorption of nucleic acid bases and amino acids on single-walled carbon and boron nitride nanotubes: a first-principles study. Journal of nanoscience and nanotechnology, 9(11), pp.6376-6380.

[36] Cho, D.Y., Eun, K., Choa, S.H. and Kim, H.K., 2014. Highly flexible and stretchable carbon nanotube network electrodes prepared by simple brush painting for cost-effective flexible organic solar cells. Carbon, 66, pp.530-538.

[37] Ma, J.L., Yin, B.C., Wu, X. and Ye, B.C., 2017. Simple and cost-effective glucose detection based on carbon nanodots supported on silver nanoparticles. Analytical chemistry, 89(2), pp.1323-1328.

[38] Antunes, M. and Velasco, J.I., 2014. Multifunctional polymer foams with carbon nanoparticles. Progress in Polymer Science, 39(3), pp.486-509.

[39] Singh, S., Bairagi, P.K. and Verma, N., 2018. Candle soot-derived carbon nanoparticles: an inexpensive and efficient electrode for microbial fuel cells. Electrochimica Acta, 264, pp.119-127.

[40] Cheng, H.M., Li, F., Su, G., Pan, H.Y., He, L.L., Sun, X. and Dresselhaus, M.S., 1998. Large-scale and low-cost synthesis of single-walled carbon nanotubes by the catalytic pyrolysis of hydrocarbons. Applied Physics Letters, 72(25), pp.3282-3284.

Received: August 05, 2025 

Volume 38 No. 12s, 2025

ISSN: 1311-1728 (printed version); ISSN: 1314-8060 (on-line version)

[41] Gao, H., Kong, Y., Cui, D. and Ozkan, C.S., 2003. Spontaneous insertion of DNA oligonucleotides into carbon nanotubes. Nano Letters, 3(4), pp.471-473.

[42] Balasubramanian, K. and Burghard, M., 2006. Biosensors based on carbon nanotubes. Analytical and bioanalytical chemistry, 385(3), pp.45.

Received: August 05, 2025 